

# Escape Kinetics of Self-Propelled Janus Particles from a Cavity: Numerical Simulations\*

Pulak Kumar Ghosh<sup>†</sup>

Department of Chemistry, Presidency University, Kolkata - 700073, India

(Dated: October 14, 2021)

We numerically investigate the escape kinetics of elliptic Janus particles from narrow two-dimensional cavities with reflecting walls. The self-propulsion velocity of the Janus particle is directed along either their major (prolate) or minor axis (oblate). We show that the mean exit time is very sensitive to the cavity geometry, particle shape and self-propulsion strength. The mean exit time is found to be a minimum when the self-propulsion length is equal to the cavity size. We also find the optimum mean escape time as a function of the self-propulsion velocity, translational diffusion, and particle shape. Thus, effective transport control mechanisms for Janus particles in a channel can be implemented.

PACS numbers: 82.70.Dd 87.15.hj 05.40.Jc

Self-propelled Janus particles (JPs) are a class of artificial microswimmers which can move by extracting energy from their suspension medium [1]. This type of particles consists of two distinct faces with different chemical or physical properties. Such two-faced particles can acquire self-propulsion by inducing chemical concentration or temperature gradients in the vicinity of active face. A number of works[2–4] show that a controllable concentration gradient can be created in some catalytic reactions on the one surface of JPs. Inhomoge-

neous light absorption[5] or magnetic excitation[6] of JPs can generate enough local temperature gradient for self-thermophoresis. Based on different self-phoretic mechanisms various kinds of self-propeller have been designed with specific goals[1, 7]

In the absence of any external force field, the motion of a self-propelled JP is directed parallel to the self-phoretic force. Gradient fluctuations or collisions with boundaries or the intrinsic rotational diffusion result in a random change of the direction of self-propulsion. Thus, self-propelled JPs exhibit time correlated active Brownian motions. Janus particles can be used as a special kind of diffusing tracer in experiments aimed at demonstrating non-equilibrium phenomena like, ratcheting[8, 9], autonomous pumps[8], absolute negative mobility[10] etc. Moreover, it would be desirable to gain control over the motion of this class of Brownian tracers, so as to use them as a “nano-robot” for applications in the medical sciences and nano-technology.

A conspicuous feature reported in earlier experiments[11] and simulations[8] is that when the mean free path ( $l_\theta$ ) of a JP is much greater than the cavity size ( $x_L$  or  $y_L$ ), the particle spends most of their time in the close vicinity of confining walls. In many practical situations, the mean free path[8] follows the condition  $l_\theta \gg x_L$  or  $y_L$ . The self-propulsive forces press JPs against walls. As a result, the JPs keep diffusing in the tangential direction under the action of translational noises until an appropriate orientational change occurs by rotational diffusion. Taking advantage of this property, JPs can be captured by placing an obstruction of appropriate shape [15], driven against an applied force[10], and rectified in asymmetric channels with high efficiency[8]. All these features make the dynamics of JPs different from living micro-swimmers[12–14] (*e.g.*, Bacteria). Living micro-swimmers change their direction whenever they encounter any obstruction on their path (run-and-tumble like dynamics[13]).

In this paper we explore how the escape kinetics of a JP out of a cavity can be controlled by tuning the self-propulsive properties as well as the shape of both,

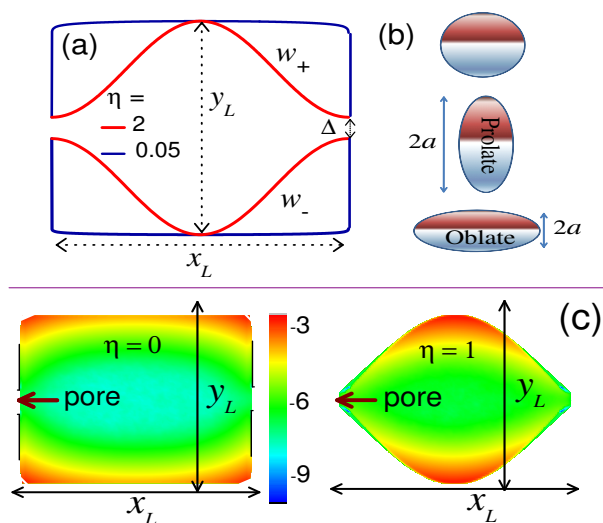


FIG. 1: (Color online) (a) Shape of the cavity for two different values of  $\eta$  using the wall profile functions,  $w_{\pm}(x)$  of Eq. (1). (b) Janus particles with various shapes. (c) Logarithmic contour plots of the stationary particle density  $P(x, y)$  in the cavities. Simulation parameters are:  $x_L = y_L = 1$ ,  $\Delta = 0.16$ ,  $a = b = 0.052$ ,  $D_0 = 0.03$ ,  $D_\theta = 0.0005$ ,  $v_0 = 1$ .

\*This paper is dedicated to Professor Deb Shankar Ray on the occasion of his sixtieth birthday.

<sup>†</sup>Email: pulak.chem@presiuniv.ac.in

the particle and confining walls. In confined systems, the boundary conditions (which are determined by the shape of particles and confining walls) govern the Brownian dynamics[17–19]. Therefore, transport control of a JP with assigned self-propulsive properties and shape can be achieved only by suitably tailoring the channel boundaries.

On the one hand, self-propulsion tries to confine JPs at some corners of the cavity. On the other hand, the translational noises tend to contrast the action of self-propulsion by broadening the localized JP densities. Moreover, effects of self-propulsion largely depend on the shape of the particle and confinement. Thus, the interplay among the translational noises, self-propulsion and particle shape produces a rich JP dynamics.

*Model.* — We consider an elongated self-propelled JP diffusing in a two-dimensional (2D) cavity (extension of conclusions to 3D is straightforward). Elongated JPs have been modelled as elliptical disks with major and minor axes  $2a$  and  $2b$ , respectively. There are a number of well-established methods to synthesize such elongated JPs[1, 2]. The walls of the cavity have been modelled by the following sinusoidal functions [depicted in Fig. 1(a)]

$$w_{\pm}(x) = \pm \frac{1}{2} \left[ \Delta + (y_L - \Delta) \sin^{\eta} \left( \frac{\pi x}{x_L} \right) \right], \quad (1)$$

where  $x_L$  and  $y_L$  are the length and width of the cavity.  $\Delta$  is the pore size through which the JPs can exit the cavity. An additional tunable geometric parameter  $\eta$  has been introduced to reproduce most of the cavity geometries investigated in the literature[17, 19–22]. For  $\eta = 2$ , the cavity represents the compartment of sinusoidally corrugated channel [17, 18]. Moreover, when  $\eta \rightarrow 0$ , the cavity reproduces the compartment of sharply corrugated channels, where geometric effects are much more prominent than the former case [19]. The bulk dynamics of a self-propelled JP can be described by the following equations[23],

$$\dot{x} = v_0 \cos \theta + \xi_x(t), \quad \dot{y} = v_0 \sin \theta + \xi_y(t), \quad (2)$$

where  $(x, y)$  denote the position of the particle center of mass. The particle diffuses under the action of self-propulsion and equilibrium thermal fluctuations. We assume that the self-propulsion velocity,  $\mathbf{v}_0$ , is oriented along either the major (for prolate) or minor (for oblate) axis of the particle. The vector  $\mathbf{v}_0$  makes an angle  $\theta$  with the  $x$ -axis of the cavity. Due to rotational diffusion of the particle,  $\theta$  changes randomly, which can be described as a Wiener process,  $\dot{\theta} = \chi_{\theta}(t)$ , with  $\langle \chi_{\theta}(t) \rangle = 0$  and  $\langle \chi_{\theta}(t) \chi_{\theta}(0) \rangle = 2D_{\theta} \delta(t)$ , where the rotational diffusion constant  $D_{\theta}$  is related to the viscosity ( $\eta_v$ ) of the medium, temperature ( $T$ ) and size of the particle. For an elliptical particle,  $D_{\theta} \propto k_B T / ab \eta_v$ . From the correlation function,  $\langle \cos \theta(t) \cos \theta(0) \rangle = \langle \sin \theta(t) \sin \theta(0) \rangle = 1/2 e^{-|t|D_{\theta}}$ , one can consider the self-propulsion velocity components,  $v_x = v_0 \cos \theta$  and  $v_y = v_0 \sin \theta$ , as the components of a 2D non-Gaussian noise  $\chi_{c,i}(t)$  with zero

mean,  $\langle \chi_{c,i}(t) \rangle = 0$ , and finite-time correlation functions,  $\langle \chi_{c,i}(t) \chi_{c,j}(0) \rangle = 2(D_c / \tau_{\theta}) \delta_{ij} e^{-2|t|/\tau_{\theta}}$ , where  $i = \{x, y\}$ , and  $D_c = v_0^2 \tau_{\theta} / 4$  with  $\tau_{\theta} = 2/D_{\theta}$  [8]. The last terms of the Eqs. (2) [ $\xi_x(t)$  and  $\xi_y(t)$ ] are the thermal noise responsible for translational diffusion of the JP.  $\xi_x(t)$  and  $\xi_y(t)$  can be modelled by Gaussian white noises with  $\langle \xi_i(t) \rangle = 0$  and  $\langle \xi_i(t) \xi_j(0) \rangle = 2D_0 \delta_{ij} \delta(t)$ , where  $D_0$  is the measure of the translational diffusion of a JP in the bulk with  $v_0 = 0$ . In the bulk, the two equations in Eqs. (2) are statistically independent, so the particle diffuses according to F urth’s law [8, 24].

The mechanisms of the translational and rotational diffusion may not be the same and therefore  $D_0$ ,  $v_0$ , and  $\tau_{\theta}$  can be treated as independent model parameters. Moreover, for the sake of simplicity, we have ignored particle-particle collisions[27] and hydrodynamic effects[26]. Despite all these simplifications, analytical calculations of the mean exit time out of a cavity is a formidable task. Therefore, we resort to numerical simulations to accomplish our goals.

We numerically estimate the mean exit time ( $T_{\text{MET}}$ ) of JPs out of the compartment of corrugated channel. The mean exit time is defined as the average time a JP requires to exit a channel compartment starting from a random initial position  $(x, y)$  and orientation ( $\theta$ ) within the cavity. The Eqs (2) have been numerically integrated under the assumption that the channel walls are perfectly reflecting and the particle-wall collisions are elastic [28]. All the results (presented in the Figs. 2-3) are obtained by ensemble averaging over  $10^4 - 10^6$  trajectories depending upon the values of parameters. We choose times in seconds and lengths in microns (see reference[29]).

*Mean exit time versus rotational diffusion.* — To understand the underlying escape mechanisms of a JP out of a cavity, we first explore  $T_{\text{MET}}$  as a function of the rotational time constant  $\tau_{\theta}$  (shown in Fig. 2). The rotational time constant is defined as the average time during which a swimming JP maintains its direction away from the walls.  $\tau_{\theta}$  is related to the bulk rotational diffusion constant as  $\tau_{\theta} = 2/D_{\theta}$ . Figure 2 shows that for  $\tau_{\theta} \rightarrow 0$ , the mean exit time attains a constant value. In the opposite limit, when  $\tau_{\theta} \rightarrow \infty$  the escape rate is approximately inversely proportional to  $\tau_{\theta}$ . Between these two limits, a minimum is observed in the  $T_{\text{MET}}$  vs.  $\tau_{\theta}$  plot. All these features can be explained by the following considerations. (i) For  $\tau_{\theta} \rightarrow 0$ , the self-propulsion velocity changes its direction instantaneously. Thus, the propulsive force acts as a zero mean white noise and its contribution to diffusion is negligibly small as  $D_0 \gg \tau_{\theta} v_0^2 / 4$ . In this regime, the  $T_{\text{MET}}$  of a spherical JP can be calculated analytically using the Zwanzig-Fick-Jacobs scheme for entropic channels [17, 30, 31] or the random walker scheme[32, 33].

$$T_{\text{MET}} = \frac{x_L^2}{8D_0} \sqrt{\frac{y_L}{\tilde{\Delta}}} \left[ 1 + \frac{\tilde{\Delta}}{y_L} \right] \quad (3)$$

where  $\tilde{\Delta} = \Delta - 2a$  is the effective pore size. Our simulation results are in good agreement with the predictions

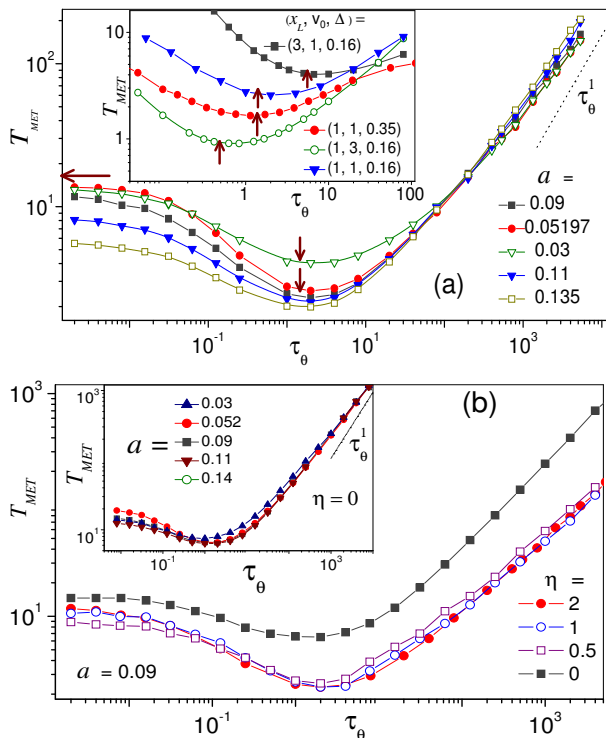


FIG. 2: (Color online) (a)  $T_{MET}$  vs.  $\tau_\theta$  for prolate, oblate and circular JPs. Semiaxes  $a$  and  $b$  are varied keeping,  $ab = 0.0027$ . Cavity parameters are:  $x_L = y_L = 1$ ,  $\Delta = 0.16$ , and  $\eta = 2$ . Other parameters are:  $v_0 = 1$  and  $D_0 = 0.03$ . The prediction of Eq. (3) has been displayed by a horizontal arrow. The dotted line is the power law  $\tau_\theta^1$  drawn for the reader's convenience. Inset present variations of  $(\tau_\theta)_m$  in  $T_{MET}$  vs.  $\tau_\theta$  plots, with  $v_0$ ,  $x_L$  and  $\Delta$  (see legends). Vertical arrows denote position of minima based on the Eq. (5). Parameters are the same as the main figure but  $a = 0.052$ .

(b)  $T_{MET}$  vs.  $\tau_\theta$  for different cavity shapes. The inset depicts the same for  $\eta = 0$  and different particle shapes. Parameters are the same as Fig. 2(a) except those are mentioned in the legends.

of Eq. (3) [indicated by an horizontal arrow in Fig. 2(a)]. However, this estimate is not valid for rod-shaped particles. Prolate JPs glide along the boundaries so that they can go through the the pore without any change of their orientation. Thus, prolate-shaped JPs take less time to exit in comparison to circular or oblate JPs.

(ii) For  $\tau_\theta \rightarrow \infty$ , the rotation of JPs against the self-propulsion is the bottleneck of the problem. To escape from the cavity, a JP requires some orientational changes for two reasons. Firstly, to be free from the sharp corners or lobes of the cavity where particles may get stuck, and secondly to be aligned to the axis of the pore of the cavity. For the parameter set of Fig. 2, the former one is the rate determining step when  $D_\theta \rightarrow 0$ . The numerical simulation of the stationary particle density  $P(x, y)$  [shown in Fig. 1(c)] corroborates this assertion. For  $\tau_\theta \rightarrow \infty$ , a power law,  $T_{MET} = A\tau_\theta^\alpha$  can be fitted to the simulation data. The pre-factor  $A$  and the exponent  $\alpha$  are indepen-

dent of the shape of the particle. But  $A$  depends on the geometry of the cavity. To exit from the cavity, if a JP needs to rotate to an angle  $\theta_1$  starting from a randomly chosen angle in between  $\theta_1$  and  $\theta_2$ , the average escape time can be estimated as[19],

$$T_{MET} \sim (\theta_2 - \theta_1)^2 / 6D_\theta = \tau_\theta(\theta_2 - \theta_1)^2 / 12 \quad (4)$$

However, our simulation results (see Fig. 2) show that  $\alpha \sim 0.9$ . This mismatch is due to the fact that the derivation of Eq. (4) tacitly assumes *free* rotational diffusion of JPs. But this is not the case practically. Self-propulsion pushes the JPs against the walls which can enhance the rotational diffusion due to the smooth curvatures of the confining walls. Even for  $\eta = 0$  the excluded-volume considerably reduces the effects of the sharp corners in the escape kinetics.

(iii) In the intermediate regime, on increasing  $\tau_\theta$  the mean exit time first decreases, then increases passing through a minimum. The orientational angle  $\theta$  of a JP may have any value between 0 to  $2\pi$ . On average, JPs drift toward the left or right exit with a velocity  $\bar{v} = v_0 \cos \pi/4$ . When the mean free path  $l_\theta^x = \tau_\theta \bar{v}$  along the cavity axis is equal to the length of the cavity, a large fraction of the trajectories can reach the boundary (also in the vicinity of the pores) without any orientational change. Moreover,  $\tau_\theta$  is not large enough to keep waiting a JP long to acquire the favorable orientations to exit from the cavity. Thus,  $T_{MET}$  vs.  $\tau_\theta$  plots exhibit a minimum at,

$$(\tau_\theta)_m = \sqrt{2} x_L / v_0 \quad (5)$$

It is apparent from Fig. 2 that the numerical analyses match fairly well with the above estimates. Figure 2(a) clearly indicates that  $(\tau_\theta)_m$  is independent of the shape of the JPs. Figure 2(b) shows that the dependence of  $T_{MET}$  on  $\tau_\theta$  is independent of the cavity shape. However, for  $\eta = 0$  the cavity possesses some sharp corners where JPs may get stuck. Becoming free from this type of stuck states is more difficult than the stuck state in a lobe of sinusoidal channel compartments. Thus, a JP takes less time to cross the compartment of smoothly corrugated channel than a sharp one.

*Mean exit time versus translational noises* — Figure 3(a) depicts  $T_{MET}$  as a function of the strength of translational noise  $D_0$ . When  $D_0$  is very small in comparison to  $v_0$ , the escape kinetics of the prolate JPs is solely guided by self-propulsion[16]. After a collision with the wall, the prolate swimmers tend to slide parallel to the wall and get out of the cavity whenever they find an opening. These swimmers slide on the walls in such a way that they do not need any further orientational change to exit the cavity. As a result, for  $D_0 \ll v_0$ , the mean exit time is independent of  $D_0$  for prolate or circular JPs. The oblate swimmers too tend to pile up against the wall and try to slide, but, due to their shape the longitudinal diffusion is suppressed[10]. Moreover, the oblate particles need assistance by thermal fluctuations  $\xi_i$  to get aligned so as to escape. This leads to a suppression of the exit

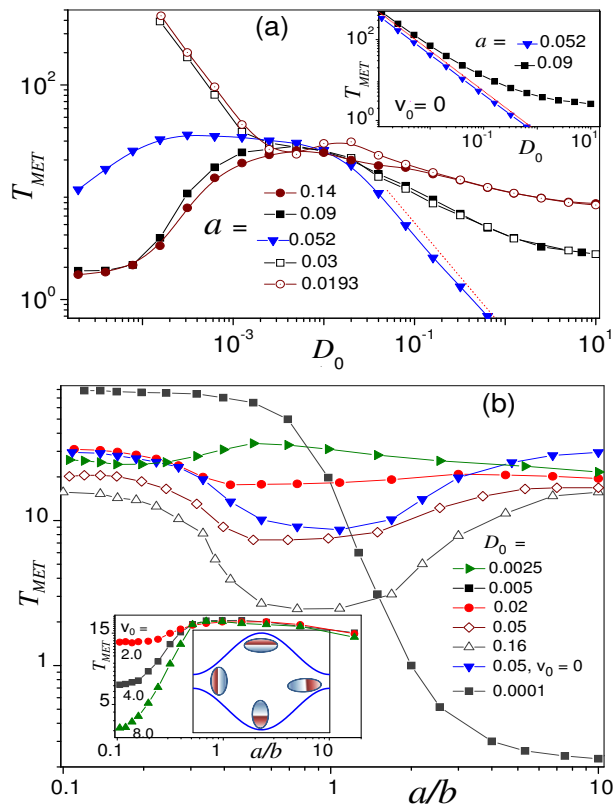


FIG. 3: (Color online) (a)  $T_{\text{MET}}$  vs.  $D_0$  for prolate, oblate and circular JPs. Compartment parameters:  $\eta = 2$ ,  $x_L = y_L = 1$  and  $\Delta = 0.16$ ; self-propulsion parameters:  $v_0 = 0.5$  and  $D_\theta = 0.01$ ; particle size:  $ab = 0.0027$ . Parameters for the inset is the same as the main figure, but  $v_0 = 0$ . The red-dotted lines are the fitting law of Eq. (3).

(b)  $T_{\text{MET}}$  vs.  $a/b$  for the different translational noise strengths. For all the curves  $v_0 = 0.5$  unless it is mentioned in the legend. Remaining parameters are same as subfigure (a).  $T_{\text{MET}}$  has been multiplied by 0.1 for the curve with  $D_0 = 10^{-4}$  to bring all the curves in the same frame. Inset:  $T_{\text{MET}}$  vs.  $a/b$  for different strength of self-propulsions (see legends). Other parameters are same as Fig.3(a). Sketch: Some most probable orientation of elongated JPs with which they approach to the opening and walls in lobes.

rate of oblate JPs with decreasing  $D_0$ . Upon increasing the intensity of  $\xi_i$ , noises start kicking the particle out of its sliding or stuck states. As a result, the escape process of oblate particles is facilitated, whereas the exit process of prolate and circular swimmers gets retarded. When  $D_0 \gg v_0$  the translational diffusion owing to  $\xi_i$  dominates over the propulsive force. In this regime, the escape rate of a circular JP is given by Eq. (3). But elongated particles cannot go through the pore unless they acquire some specific orientational angles by rotational diffusion. Thus, the exit rate of prolate or oblate JPs becomes insensitive to  $D_0$  for  $D_0 \rightarrow \infty$  and the asymptote can be determined by making use of Eq. (4).

*Mean exit time versus particle shapes* — To better understand the interplay between the translational noise

strength and the particle shape in the escape kinetics, we estimate  $T_{\text{MET}}$  as a function of  $a/b$  keeping  $ab = \text{fixed}$  [see Fig 3(b)]. For large  $D_0$  or in the absence of self-propulsion the  $T_{\text{MET}}$  vs.  $a/b$  plots take a symmetric U-shape with two horizontal asymptotes. In this regime,  $T_{\text{MET}}$  has a minimum for  $a = b$  (circular JPs) and maximum for  $a \gg b$  or  $a \ll b$  (elongated JPs). Upon decreasing the noise intensity  $D_0$  the curves in Fig. 3(b) become asymmetric and the exit time for the prolate JPs become different from the oblate ones. This result can be understood based on the arguments of the preceding paragraphs. The most surprising result is that circular particles take the longest time to escape from the cavity, while, in certain  $D_0$  regimes, the oblate ones take the shortest. This attributes to the trapping of the particles at the lobes of the cavity [see sketch in the inset of Fig. 3(b)]. The sticking mechanism and the stuck states have some interesting features to note:

(i) For  $D_0 \rightarrow 0$ , self-propulsion tends to press the particle against the walls, while, interactions with walls having a smooth curvature guide the particle to slide on it. Thus, the particle does not get stuck in the lobes of the cavity and rotation of the particles against the self-propulsion is the slowest step. Therefore, the prolate or circular JPs can exit much faster than the oblate ones. The  $T_{\text{MET}}$  vs.  $a/b$  plot for  $D_0 = 10^{-4}$  in Fig. 3(b) corroborates this assertion. Also in the opposite limit,  $D_0 \gg v_0$  the sticking mechanism has little impact on the escape dynamics as the noises kick the particle out of its sliding or stuck states. Between these two limits, there is an intermediate regime of  $D_0$  where the effects of trapping at the lobes become important in the escape kinetics.

(ii) As anticipated based on geometric considerations regarding the most probable orientation of the particles near walls [see the sketch in the inset of Fig.3(b)], a circular disk get stuck in the lobes most tightly and an oblate one rather weakly. Thus, in the presence of a very strong self-phoretic force oblate particles can escape from the cavity much faster than the circular or prolate ones.

*In conclusion*, depending upon the relative strength of the propulsion and the translational noise, two kinds of noise-activated processes, (a) rotation against the propulsive force and (b) noise-induced hopping from the trapped states in lobes or sharp corners, play the central role in the JPs escape kinetics. When acquiring an appropriate orientation to exit is the rate determining step, a prolate JP has an order of magnitude larger escape rate than the particles with other shapes. On the other hand, when the trapping mechanism dictates the escape kinetics, oblate JPs require less time to exit from a cavity in comparison to prolate or circular ones. Moreover, the escape rate from a cavity can be maximized by adjusting the self-propulsion strength in such a way that the mean free path of the JP matches with the cavity size. The self-propulsion velocity of a JP driven by chemical reactions can be tuned by changing concentrations of reactants or catalysts[2–4]. Again, in the experimental set up of light-driven JPs[11], one can easily control the self-

propulsion velocity by adjusting the intensity of light. Therefore, our simulation results can be used to design most efficient JPs for targeted drug delivery, and many applications in natural and artificial devices.

Acknowledgments – I wish to thank Professor F. Marchesoni (Universita di Camerino, Italy) and Dr. D. P. Chatterjee (Presidency University, India) for critical comments and suggestions.

- 
- [1] S. Jiang and S. Granick (eds.), *Janus Particle Synthesis, Self-Assembly and Applications* (RSC, Cambridge, 2012).
- [2] W. F. Paxton, S. Sundararajan, T. E. Mallouk, and A. Sen, *Angew. Chem. Int. Ed.* **45**, 5420 (2006).
- [3] J. G. Gibbs and Y.-P. Zhao, *Appl. Phys. Lett.* **94**, 163104 (2009).
- [4] J. R. Howse, R. A. L. Jones, A. J. Ryan, T. Gough, R. Vafabakhsh, and R. Golestanian, *Phys. Rev. Lett.* **99**, 048102 (2007).
- [5] H. R. Jiang, N. Yoshinaga, and M. Sano, *Phys. Rev. Lett.* **105**, 268302 (2010).
- [6] L. Baraban, R. Streubel, D. Makarov, L. Han, D. Kar-naushenko, O. G. Schmidt, and G. Cuniberti, *ACS Nano* **7**, 1360 (2013).
- [7] M. Y. Matsuo and S. Sano, *J. Phys. A: Math. Theor.* **44** 285101 (2011).
- [8] P. K. Ghosh, V. R. Misko, F. Marchesoni, and F. Nori, *Phys. Rev. Lett.* **110**, 268301 (2013).
- [9] B.-Q. Ai and J.-C. Wu *J. Chem. Phys.* **140**, 094103 (2014).
- [10] P. K. Ghosh, P. Hänggi, F. Marchesoni, and F. Nori *Phys. Rev. E* **89**, 062115 (2014).
- [11] G. Volpe, I. Buttinoni, D. Vogt, H.-J. Kümmerer, and C. Bechinger, *Soft Matter*, **7**, 8810 (2011).
- [12] H.C. Berg and D.A. Brown, *Nature* **239**, 500504 (1972); T.L. Min, P.J. Mears, L.M. Chubiz, C.V. Rao, I. Golding, and Y.R. Chemla, *Nature Methods* **6**, 831 (2009).
- [13] J. Tailleur and M. E. Cates, *Phys. Rev. Lett.* **100**, 218103 (2008); R. W. Nash, R. Adhikari, J. Tailleur, and M. E. Cates, *Phys. Rev. Lett.* **104**, 258101 (2010)
- [14] R. Allena and D. Aubry, *J. Theo. Biology* **306**, 15 (2012).
- [15] A. Kaiser, K. Popowa, H. H. Wensink, and H. Löwen, *Phys. Rev. E* **88**, 022311 (2013).
- [16] from a dimensional point of view  $D_0$  should be compared with  $v_0 x_L$ , which in the present case equals one.
- [17] P.S. Burada, P. Hänggi, F. Marchesoni, G. Schmid, and P. Talkner, *ChemPhysChem* **10**, 45 (2009).
- [18] P. K. Ghosh, P. Hänggi, F. Marchesoni, F. Nori, and G. Schmid *Phys. Rev. E* **86**, 021112 (2012); *Europhys. Lett.* **98**, 50002 (2012).
- [19] M. Borromeo *et al.*, *J. Chem. Phys.* **134**, 051101 (2011); P. K. Ghosh, F. Marchesoni, S. Savel'ev, and F. Nori, *Phys. Rev. Lett.* **104**, 020601 (2010); P. K. Ghosh, R. Glavey, F. Marchesoni, S. E. Savelev, and F. Nori, *Phys. Rev. E* **84**, 011109 (2011).
- [20] B. Q. Ai and L. G. Liu, *Phys. Rev. E* **74**, 051114 (2006); B. Q. Ai and L. G. Liu, *J. Chem. Phys.* **126**, 204706 (2007); *J. Chem. Phys.* **128**, 024706 (2008).
- [21] P. K. Ghosh and F. Marchesoni, *J. Chem. Phys.* **136**, 116101 (2012).
- [22] D. Mondal and D. S. Ray, *Phys. Rev. E* **82**, 032103(2010); D. Mondal *Phys. Rev. E* **84**, 011149 (2011).
- [23] S. van Teeffelen and H. Löwen, *Phys. Rev. E* **78**, 020101 (2008).
- [24] Y. Fily and M.C. Marchetti, *Phys. Rev. Lett.* **108**, 235702 (2012).
- [25] M. Mijalkov and G. Volpe, *Soft Matter*, **9**, 6376 (2013).
- [26] M. Ripoll, P. Holmqvist, R.G. Winkler, G. Gompper, J.K.G. Dhont, and M.P. Lettinga, *Phys. Rev. Lett.* **101**, 168302 (2008).
- [27] I. Buttinoni, J. Bialke, F. Kümmel, H. Löwen, C. Bechinger, and T. Speck, *Phys. Rev. Lett.* **110**, 238301 (2013).
- [28] P. Hänggi, F. Marchesoni, S. Savelev, and G. Schmid, *Phys. Rev. E* **82**, 041121 (2010).
- [29] Unit of parameters:  $(x_L, y_L, \Delta, a, b, l_\theta)\mu\text{m}$ ,  $(T_{\text{MET}}, \tau_\theta)$  second,  $v_0 \mu\text{m/s}$ , and  $D_0 \mu\text{m}^2/\text{s}$
- [30] M. H. Jacobs, *Diffusion Processes* (Springer, NY, 1967).
- [31] R. Zwanzig, *J. Phys. Chem.* **96**, 3926 (1992).
- [32] L. Bosi *et al.*, *J. Chem. Phys.* **137**, 174110 (2012)
- [33] A. M. Berezhkovskii, L. Dagdug, Yu. A. Makhnovskii, and V. Yu. Zitserman, *J. Chem. Phys.* **132**, 221104 (2010); Yu. A. Makhnovskii, A. M. Berezhkovskii, L. V. Bogachev, and V. Yu. Zitserman, *J. Phys. Chem. B* **115**, 3992 (2011).